

Mapping multiple photonic qubits into and out of one solid-state atomic ensemble

Imam Usmani, Mikael Afzelius,* Hugues de Riedmatten, and Nicolas Gisin
Group of Applied Physics, University of Geneva, CH-1211 Geneva 4, Switzerland
 (Dated: July 22, 2018)

The future challenge of quantum communication are scalable quantum networks, which require coherent and reversible mapping of photonic qubits onto stationary atomic systems (quantum memories). A crucial requirement for realistic networks is the ability to efficiently store multiple qubits in one quantum memory. Here we demonstrate coherent and reversible mapping of 64 optical modes at the single photon level in the time domain onto one solid-state ensemble of rare-earth ions. Our light-matter interface is based on a high-bandwidth (100 MHz) atomic frequency comb, with a pre-determined storage time $\gtrsim 1 \mu\text{s}$. We can then encode many qubits in short $< 10 \text{ ns}$ temporal modes (time-bin qubits). We show the good coherence of the mapping by simultaneously storing and analyzing multiple time-bin qubits.

Quantum communication [1] offers the possibility of secure transmission of messages using quantum key distribution (QKD) [2] and teleportation of unknown quantum states [3]. Quantum communication relies on creation, manipulation and transmission of qubits in photonic channels. Photons have proven to be robust carriers of quantum information. Yet, the transmission of photons through a fiber link, for instance, is inherently a lossy process. This leads to a probabilistic nature of the outcome of experiments. In large-scale quantum networks [4] the possibility of synchronizing independent and probabilistic quantum channels will be required for scalability [5, 6]. A quantum memory enables this by momentarily holding a photon and then releasing it when another part of the network is ready. In order to reach reasonable rates in a realistic network it will be necessary to use multiplexing [7], which requires quantum memories capable of storing many single photons in different modes.

A quantum memory requires a coherent medium with strong coupling to a light mode. Strong and coherent interactions can be found in ensembles of atoms [8], for instance alkali atoms or rare-earth (RE) ions doped into crystals. The latter are attractive for quantum storage applications, as they provide solid-state systems with a large number of stationary atoms with excellent coherence properties. Optical coherence times of up to milliseconds [9] and spin coherence times $> \text{seconds}$ [10] have been demonstrated at low temperature ($\lesssim 4 \text{ K}$).

A quantum memory also requires a scheme for achieving efficient and reversible mapping of the photonic qubit onto the atomic ensemble. Techniques investigated include stopped light based on electromagnetically induced transparency (EIT) [11–13], Raman interactions [14–16] or photon-echo based schemes [17–21]. Much progress has been made in terms of quantum memory efficiency [13, 22], and storage time [23, 24]. Storage of multiple qubits is challenging, however, because it requires a quantum memory that can store many optical modes into which qubits can be encoded. Note that each pair of modes can encode a different qubit, or more gener-

ally, d modes encode a qudit. A mode can be defined in time [7], space [25], or frequency. Time multiplexing as used in classical communication has the great advantage of requiring only a single spatial mode [20, 26], hence a single quantum memory. Moreover, temporal modes can be used to define time-bin qubits [1], which are widely used in fiber-based quantum communication due to their resilience against polarization decoherence in fibers.

This type of temporal multimode storage is difficult, however, due to the scaling of the number of stored modes N_m as a function of optical depth d of the storage medium [20, 26]. For EIT and Raman interactions N_m scales as \sqrt{d} [26], making it very difficult to store many modes. Recently we proposed [20] a multimode storage scheme based on atomic frequency combs (AFC) with high intrinsic temporal multimode capacity [20, 26]. Using this method we recently demonstrated [21] that a weak coherent state $|\alpha\rangle_L$ with mean photon number $\bar{n} = |\alpha|^2 < 1$, can be coherently and reversibly mapped onto a YVO_4 crystal doped with neodymium ions. Later experiments [27–29] in other RE-doped materials have improved the overall storage efficiency (35%) and storage time ($20 \mu\text{s}$). Yet, in these experiments at most 4 modes have actually been stored at the single photon level, thus the predicted [20, 26] high multimode capacity has yet to be shown experimentally.

RESULTS

Here we demonstrate reversible mapping of 64 temporal modes containing weak coherent states at the single photon level onto one atomic ensemble in a single spatial mode using an AFC-based light-matter interface [20]. An AFC is based on a periodic modulation (with periodicity Δ) of the absorption profile of an inhomogeneously broadened optical transition $|g\rangle \rightarrow |e\rangle$ (see Fig. 1). The modulation should ideally consist of sharp teeth (with full-width at half-maximum γ) having high peak absorption depth d , cf. Figure 1b. Such a modulation can be created by optical pumping techniques (see Figure 1 and

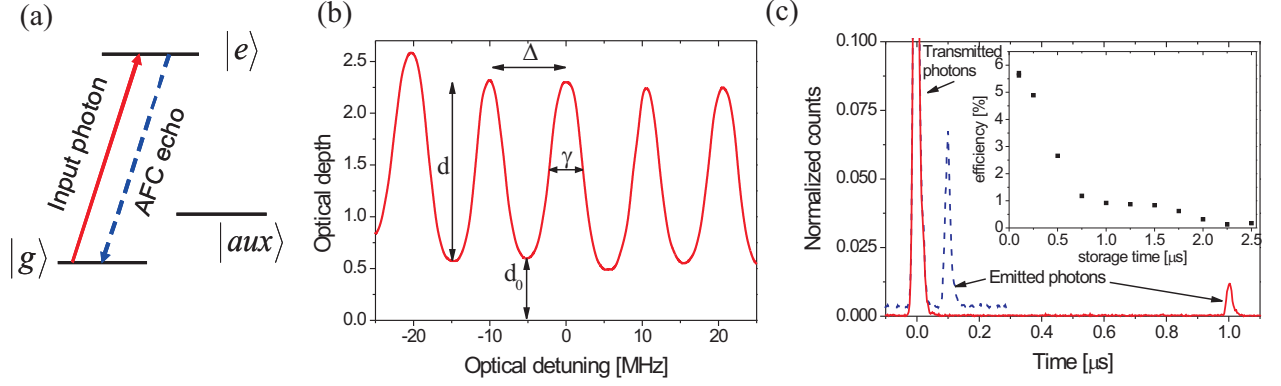


FIG. 1: (a) Simplified level scheme of the Nd ions doped into Y_2SiO_5 . We use the optical transition at 883nm between the $^4\text{I}_{9/2}$ ground state and $^4\text{F}_{3/2}$ excited state. The former is split into two Zeeman levels by a 0.3 Tesla magnetic field ($|g\rangle$ and $|aux\rangle$). The experiment is performed on $|g\rangle$ - $|e\rangle$ where the absorption profile is shaped into an AFC by optically pumping atoms into $|aux\rangle$. The basic idea is to send in a pulse sequence on $|g\rangle$ - $|e\rangle$ that has a periodic spectral density (due its Fourier spectrum). Some of the excited atoms have a certain probability to spontaneously de-excite to $|aux\rangle$. The atoms left behind in $|g\rangle$ form the grating (see panel (b)). To build up a deep grating the sequence is repeated many times (up to the timescale of the population relaxation between $|g\rangle$ and $|aux\rangle$). More details on the preparation can be found in the Supplementary Information. (b) An example of a generated comb with periodicity $\Delta=10$ MHz. The relevant AFC parameters defined in the text are indicated. (c) Mapping of weak coherent states with $\bar{n} = 0.5$ (in a single temporal mode) onto the Nd-doped crystal. Shown are two different experiments with $\Delta=10$ MHz (dashed line offset vertically) and 1 MHz (solid line). The photons that are transmitted without being absorbed are detected at $t=0$, while the absorbed and re-emitted photons are detected around $t = 1/\Delta$. The vertical scale has been normalized such that it yields efficiency. Inset: The overall write and read efficiency as a function of $1/\Delta$.

Methods). This requires, however, an atomic ensemble with a static inhomogeneous broadening and many independently addressable spectral channels. This can be found in RE-doped solids where inhomogeneous broadening is of order 1-10 GHz and the homogeneous linewidth is of order 1-100 kHz when cooled $< 4\text{K}$. When a weak photonic coherent state $|\alpha\rangle_L$ with $\bar{n} < 1$ is absorbed by the atoms in the comb, the state of the atoms can be written as $|\alpha\rangle_A = |G\rangle + \alpha|W\rangle + O(\alpha^2)$. Here $|G\rangle = |g_1 \cdots g_N\rangle$ represents the ground atomic state and

$$|W\rangle = \sum_n c_n e^{i2\pi\delta_n t} e^{-ikz_n} |g \cdots e_n \cdots g\rangle \quad (1)$$

represents one induced optical excitation delocalized over all the N atoms in the comb. In Eq. (1) z_n is the position of atom n , k is the wave-number of the single-mode light field, δ_n the detuning of the atom with respect to the laser frequency and the amplitudes c_n depend on the frequency and on the spatial position of the particular atom n . The initial (at $t=0$) collective strong coupling between the light mode and atoms is rapidly lost due to inhomogeneous dephasing caused by the $\exp(i2\pi\delta_n t)$ phase factors. If we assume that the peaks are narrow as compared to the periodicity (i.e. a high comb finesse $F = \Delta/\gamma$), then $\delta_n \approx m_n \Delta$ and the W state will rephase after a pre-programmed time $1/\Delta$. The rephased collective state W will cause a strong emission in the forward direction (as defined by the absorbed light).

This type of photon-echo emission is also observed in accumulated or spectrally programmed photon echoes [30–33], which inspired our proposal. Spectral atomic gratings have also been proposed [34] and demonstrated [35] for coherent optical delay of streams of strong classical pulses. The interest in spectral gratings was recently renewed in the context of quantum memories, when it was realized how to achieve a much more efficient spectral grating than previously possible. This is possible due to the highly absorbing and sharp peaks in the AFC structure [20]. In practice the finite finesse of the comb still needs to be accounted for, which causes a partial loss of the collective state. But in Ref. [20] we show theoretically that $F=10$ induces a negligible loss, which in combination with a high optical depth d makes the AFC scheme very efficient. High-efficiency mapping using high-finesse combs have been shown experimentally [27, 29]. These experiments and the present work stores light for a pre-determined time given by $1/\Delta$. We thus emphasize that we also proposed [20] and experimentally demonstrated [28] a way to achieve on-demand readout by combining AFC with spin-wave storage. On-demand readout is a crucial resource for applications in quantum networks in order to render different quantum channels independent.

The multimode property of an AFC memory can easily be understood qualitatively. For a periodicity Δ and N_p peaks, its total bandwidth is of order $\sim N_p \Delta$ meaning

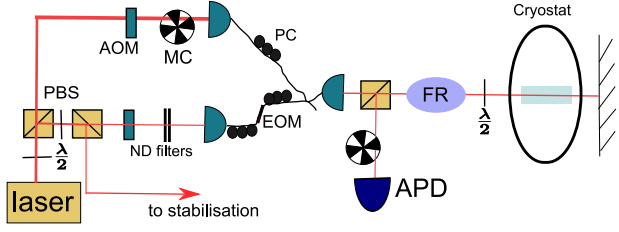


FIG. 2: The output from a frequency-stabilized ($<100\text{kHz}$) diode laser was split into two beams using a polarization beam splitter (PBS). Each beam could be amplitude, frequency and phase modulated using a double-pass acousto-optic modulators (AOM). One beam was used for creating the preparation pulses (see text), and the other one for creating the weak pulses to be stored (strongly attenuated using neutral density (ND) filters). In the weak path an additional electro-optic amplitude modulator (EOM) was used to create short input pulses for the multimode storage experiments. The paths were mode overlapped using a fiber-coupled beam combiner. The light was sent through the crystal, again in free space, in a double-pass setup using a Faraday rotator (FR) and a PBS. The output light was collected with a multimode fiber and detected by an Si single-photon counter (APD). Two synchronized mechanical choppers (MC) blocked the detector during the preparation sequence and blocked the preparation beam during the storage sequence, respectively. See Supplementary Information for more details.

that a pulse of duration $\tau \sim 1/(N_p\Delta)$ can be stored. The multimode capacity stems from the fact that the grating can absorb a train of weak pulses before the first pulse is re-emitted after $T = 1/\Delta$ (cf. Fig. 1c). This simple calculation gives a multimode capacity $N_m \propto T/\tau \propto N_p$. Thus a comb with many peaks N_p allows us to create a highly multimode memory in the temporal domain. In this context RE-doped solids are particularly interesting due to their high spectral channel density.

Here we work with a neodymium-doped Y_2SiO_5 crystal having a transition wavelength at 883 nm with good coherence properties (see Methods for the spectroscopic information). This wavelength is convenient since we can work with a diode laser and Si based single photon counters having low noise (300 Hz) and high efficiency (32%).

The comb is prepared on the $|g\rangle - |e\rangle$ transition by frequency selectively pumping atoms into an auxiliary state $|aux\rangle$ (see Fig. 1). There are different techniques for achieving this. For instance, by creating a large spectral hole, and then transferring back atoms from an auxiliary state to create a comb, as used in [28]. Here we use a similar technique to [21], where a series of pulses separated by a time τ pump atoms from $|g\rangle$ to $|aux\rangle$ (through $|e\rangle$) with a power spectrum having a periodicity $1/\tau = \Delta$. This technique is also frequently used in accumulated photon echo techniques [30, 35]. Here each pulse sequence consisted of three pulses where the central pulse is π -dephased, which has a power spectrum with "holes" (see Fig. 3c). A straightforward calculation

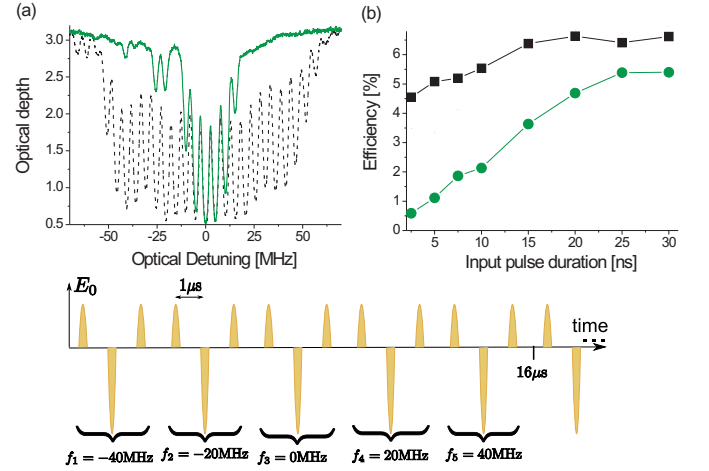


FIG. 3: (a) Experimental combs created using preparation sequences with either single (solid line) or five (dashed line) simultaneous pump frequencies. The frequency shifted sequences allows us to enlarge the frequency range over which the optical pumping is efficient and thereby creating a wide 100 MHz comb. (b) Efficiency as a function of the duration (FWHM) of the input pulse for a single (circles) and five (squares) frequency preparation. As the duration decreases the bandwidth of the input pulse increases. The decrease in efficiency for short pulses is due to bandwidth mismatch for large bandwidths when using a single preparation frequency. This experiment clearly illustrates the gain in bandwidth in the extended preparation sequence for which only a small decrease in efficiency is observed. (c) Pulse sequence for atomic frequency comb preparation (see text). In order to increase the bandwidth, the pulses are repeated with shifted frequencies. This pulse sequence was used for most of our experiments. Here it creates a comb of 100MHz bandwidth and a periodicity of 1MHz. The total sequence takes $16\mu\text{s}$ and it is repeated around 2000 times in order to prepare the AFC.

shows that the width of the holes in the power spectrum decreases with the number of pulses in the sequence. In this experiment three pulses were enough to reach the optimal comb finesse ($F \approx 3$) to achieve the maximal efficiency for a given optical depth (see Methods). Note that the sum of the amplitudes of the side pulses (here two) should correspond to the amplitude of the central π -dephased pulse, in order to obtain the appropriate power spectrum. This rule also holds for sequences with more pulses. To increase the depth of the comb the sequence was repeated 2000 times. More details can be found in the Supplementary Information.

The experimental sequence is divided into two parts: the preparation of the AFC (cf. above) and the storage of the weak pulses. The preparation lasts 100 ms, which is followed by a delay of 5 ms ($\approx 17T_1$) to avoid fluorescence noise from atoms left in the excited state. During the storage sequence, 1000 independent trials are performed at a repetition rate of 200 kHz. The entire sequence preparation plus storage is then repeated with a repetition rate of 5 Hz. An overview of the experimental

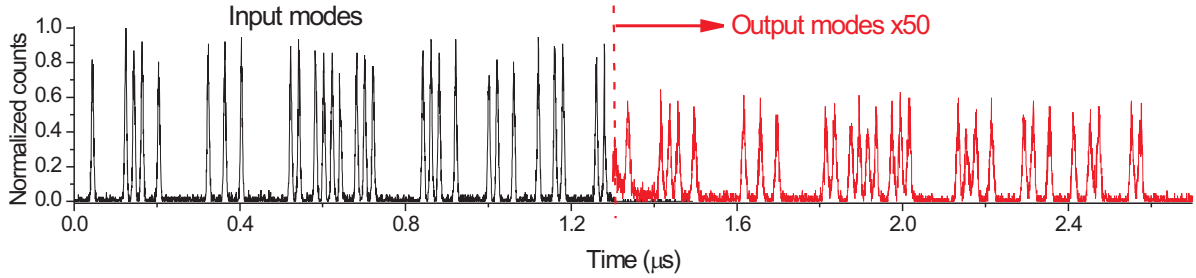


FIG. 4: Storage of an input state composed of 64 temporal modes. The input (left part) is a random sequence of full and empty time bins, where the mean photon number in the full ones is $\bar{n} \lesssim 1$. The output (right part) clearly preserves the amplitude information to an excellent degree. The pre-determined storage time was $T=1.32 \mu\text{s}$, the duration of the input $1.28 \mu\text{s}$, the mode separation 20 ns and the mode duration (FWHM) 5 ns. The output has been multiplied with a factor of 50 for clarity. The average storage and retrieval efficiency was here 1.3%. Other examples of multimode storage, e.g. with all time bins filled can be found in the Supplementary Information.

set up is shown in Fig. 7.

In Fig. 1c we show storage experiments with pre-determined storage times of $T=100\text{ns}$ and $1\mu\text{s}$, for a single temporal mode. The overall in-out mapping efficiencies, defined as the ratio of the output pulse counts to the input pulse counts, are $\sim 6\%$ and $\sim 1\%$ respectively (see inset of Fig. 1c). In the Methods section we present a theoretical analysis of the efficiency performance. The efficiency for single-mode storage is currently lower than has been achieved in the best-performance single-mode memories, e.g. [13, 16, 19, 27, 29]. But as explained later our interface compares very favorably to these experiments in terms of potential multimode storage efficiency.

The main goal of the present work is to demonstrate high multimode storage, as theoretically predicted in [20, 26]. Following the discussion above, we should maximize the number of peaks in the comb. This can be done by increasing the density of peaks in a given spectral region (i.e. increasing the storage time T) or by changing the width of the AFC (i.e. increasing the bandwidth). Here we fix the storage time to $T=1.3 \mu\text{s}$ where we reach an efficiency of $\gtrsim 1\%$ and concentrate our efforts on increasing the bandwidth. The spectral width of the grating is essentially given by the width of the power spectrum of the preparation sequence, which here results in a width of about 20-30 MHz. We can however substantially increase the total width by inserting more pulses in the preparation sequence, which are shifted in frequency (see Methods). We thus optically pump atoms over a much larger frequency range. Note that the frequency shift should be a multiple of Δ in order to form a grating without discontinuities. In this way we managed to extend the bandwidth of the interface to 100 MHz as shown in Fig. 3a, without significantly affecting the AFC echo efficiency. This is illustrated in Figure 3b, where we show storage efficiency as a function of the duration of the input pulse when the preparation sequence contains

a single or five frequencies. The maximum bandwidth allows us to map short <10 ns pulses into the memory.

In addition to the present motivation for multimode storage, a large bandwidth is equally interesting for interfacing a memory with non-classical single-photon or photon pair sources. These usually have large intrinsic bandwidth which requires extensive filtering for matching bandwidths. In the present case our extended bandwidth ($\times 5$) would require a corresponding factor of less

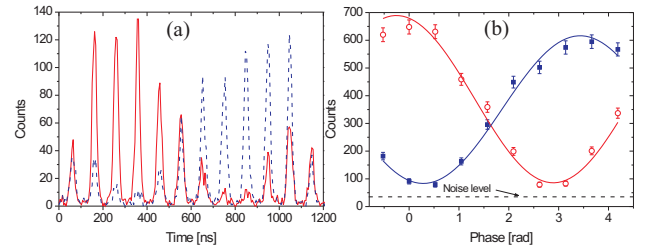


FIG. 5: The coherence of the multimode storage was measured via an interference measurement. (a) The output signal (solid line) generated by the double-AFC scheme (see text), which causes an interference between consecutive modes. The input sequence (not shown) is a series of weak coherent states ($\bar{n} \approx 1.8$) of equal amplitude ($c_k^2 = c_m^2$) where the relative phase difference between modes $\phi_{k+1} - \phi_k$ ranges from $-\pi/6$ to $8\pi/6$ with a step of $\pi/6$. This allows us to capture a complete interference fringe in one measurement. It also clearly demonstrates the preservation of coherence over the complete multimode output. By changing the detuning of the centre of the second AFC with respect to the carrier frequency of the light, we can impose an additional relative π phase [20] on the corresponding output (see Supplementary Information). This shifts the interference fringe with half a period (dashed line). (b) The corresponding net interference visibilities are $86\% \pm 3\%$ (open circles) and $85\% \pm 3\%$ (filled squares), with detector noise (dashed line) subtracted. The uncorrected raw visibilities were $78\% \pm 3\%$ and $76\% \pm 2\%$.

filtering.

We show the high multimode capacity of our interface by storing 64 temporal modes during a pre-determined time of 1.3 microseconds (see Fig. 4), with an overall efficiency of 1.3%. This capacity is more than an order of magnitude higher than previously achieved for multiplexing a quantum memory in a single spatial mode [16, 21]. As shown we can store a random sequence of weak coherent states. Storage of random trains of single photon states has been proposed for multiplexing long-distance quantum communication systems based on so called quantum repeaters [5, 6]. The maximum rate of communication would then be proportional to the number of modes that can be stored [7]. Our experiment clearly shows the gain that can be made using an AFC-based quantum memory. It thus opens up a route towards achieving efficient quantum communication using quantum repeaters.

It is now possible to use consecutive temporal modes, e.g. modes $|k\rangle$ and $|k+1\rangle$, to encode time-bin qubits $c_k|k\rangle + c_m e^{i\phi_{km}}|m\rangle$, in which case a good coherence between modes is crucial. The coherence can be measured by preparing superposition states and performing projective measurements using an interferometric set up. Projective measurements on time-bin qubits is usually performed using an unbalanced Mach-Zehnder interferometer (MZI) where consecutive time-bin are interfering [1]. We can perform the same task with our light-matter interface by using a double-AFC scheme (with Δ_1 and Δ_2) as shown in [21]. In short, the difference in delay $1/\Delta_1 - 1/\Delta_2$ plays the role of the delay in a unbalanced MZI. We observe excellent coherence over all modes with an average visibility of $V = 86\% \pm 3\%$, see Fig. 5, corresponding to a conditional qubit fidelity of $F = (1 + V)/2 \approx 93\%$.

To further illustrate our ability to store multimode light states we create a light pulse with a random amplitude modulation. As shown in Fig. 6 we can faithfully store this kind of light pulses. The possibility of storing weak arbitrary light states using photon-echo based schemes was pointed out already by Kraus et al. [18]. We believe that this work, where complex phase and amplitude information are reversible and coherently mapped onto one atomic ensemble, is the first experimental realization showing these properties at the single photon level.

DISCUSSION

For multimode storage the efficiency of our interface would outperform the current EIT and Raman based quantum memories in homogeneously broadened media, although impressive efficiencies have been achieved for single-mode storage [8, 13, 22]. This is due to the poor scaling of the efficiency as a function of the number of

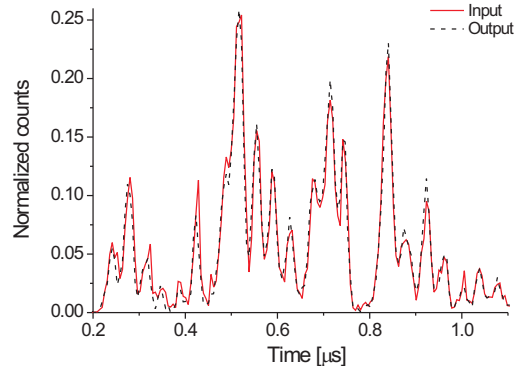


FIG. 6: Mapping of a 1 μ s long input pulse with randomly varying amplitude. As seen the overlap between the normalized input (dashed line) and output (solid line) pulses is excellent. The total average number of photons in the input pulse is $\bar{n} \approx 4$

modes for a given optical depth [26]. It also compares favorably to the recent few modes storage experiment [16] using the gradient echo memory (GEM), another echo based storage scheme, also due to the scaling of mode capacity for a given optical depth ($N_m \sim d$) [7, 26]. Still, an increase in storage efficiency and on-demand read out is necessary for applications in quantum communication.

The next grand challenge is to combine multimode storage, high efficiency [29] and on-demand read out [28] in one experiment. The immediate efforts will most probably be devoted to praseodymium and europium-doped Y_2SiO_5 crystals, where the ground state manifold has the necessary number of spin levels (three levels) for implementing the on-demand readout. The recent achievements in Pr-doped Y_2SiO_5 crystals are very encouraging [28, 29], although the bandwidth was limited to a few MHz due to the hyperfine level splitting. Europium-doped Y_2SiO_5 has the potential of offering higher bandwidths (up to 70 MHz) and narrower comb peaks, which results in higher multimode capacity [20]. In order to exploit the high-bandwidth results reported in this work, using neodymium-doped crystals, one needs to find a third spin level with a long spin coherence lifetime. An interesting path forward is to investigate neodymium isotopes with a hyperfine structure (^{143}Nd and ^{145}Nd) [36]. Recent results on a similar system [37], $^{167}\text{Er}^{3+}:\text{CaWO}_4$, show coherence times approaching 100 μ s for hyperfine transitions. Clearly this path requires extensive spectroscopic studies in order to optimize the spin population and coherence lifetimes. But it is very interesting since it opens up several material candidates (e.g. doped with Erbium [38] and Neodymium) for quantum memory applications.

To summarize we have demonstrated the reversible mapping of up to 64 optical temporal modes at the single

photon level onto one solid state atomic ensemble. We have demonstrated that the quantum coherence of the stored modes is preserved to a high extent. The different modes can then be used to encode multiple time-bin photonic qubits. Alternatively, they could also be considered as high-dimensional qudits states. This opens up possibilities to store higher dimensional quantum states such as entangled qudits encoded in time bin bases. Our experiment opens the way to multi-qubit quantum memories, which are a crucial requirement for realistic quantum networks.

METHODS

Sample

The sample is a 10mm long neodymium-doped yttrium orthosilicate crystal ($\text{Nd}^{3+}:\text{Y}_2\text{SiO}_5$) with a low Nd^{3+} concentration of 30 ppm. The inhomogeneous broadening of the $^4\text{I}_{3/2}-^4\text{F}_{3/2}$ absorption line is around 6GHz and the optical depth 1.5 for this sample. By using a double-pass set up through the crystal we could increase the optical depth to 3. We measured an excited state lifetime of $T_1=300\mu\text{s}$ using fluorescence spectroscopy and stimulated photon echoes. With conventional photon echoes (two-pulse) we measure a homogeneous linewidth of 3.4kHz ($T_2 = 92.7\mu\text{s}$). Each level is a Kramer's doublet which split into two spin states in a magnetic field. For the field orientation used in this experiment we measured g factors of $g_g = 2.6$ and $g_e = 0.5$. In a 300mT magnetic field, the excited states were separated with 2GHz. We measured a ground state Zeeman population relaxation lifetime, by spectral hole burning (SHB), of around $T_{1Z}=100\text{ms}$. In the SHB measurements we also observed a superhyperfine interaction of Nd ions with yttrium. This causes additional spectral side holes at around 640kHz (for the present magnetic field), thus the effective homogeneous linewidth is around 1 MHz. This was our main limitation for the efficiency of our light-matter interface since it affected our ability to create a good comb for the longer storage times ($1/\Delta \approx 1\mu\text{s}$).

Storage efficiency analysis

The efficiency can be calculated theoretically using the formula [20, 21] $\eta \approx (d/F)^2 e^{-d/F} e^{-7/F^2} e^{-d_0}$. The different terms can be given a qualitative understanding. The first term represents the collective coupling, the second the re-absorption of the re-emitted light, the third is an intrinsic dephasing factor due to the finesse and the last term a loss due to an absorption background d_0 . For the comb with $\Delta=10\text{MHz}$ we measure $d \approx 1.7$, $F \approx 2.7$ and $d_0 \approx 0.5$ (see Fig. 1b), resulting in a theoretical efficiency of $\eta \approx 5\%$ in close agreement with the experiment (see Fig. 1c). The major limiting factor here is d_0 (caused by imperfect preparation of the comb) and then the optical depth of the comb d (the finesse being close to optimum for this d [20]). The decrease in efficiency for longer storage times (see inset of Fig. 1c) is principally due to an increase in the background absorption d_0 and an accompanying decrease in the peak absorption d . This in turn is caused by the effective spectral resolution of 1 MHz in the optical pumping, which is a limitation of the present material (see Methods above). However, the storage efficiency is between one and two orders of magnitude higher than what we achieved in the material $\text{Nd}:\text{YVO}_4$ [21], which we attribute to an improvement in optical pumping in this Nd-doped material.

Acknowledgements We acknowledge financial support from the Swiss NCCR Quantum Photonics, the EC projects Qubit Applications (QAP) and ERC Advanced Grant (QORE). We also acknowledge useful discussions with Christoph Simon and Nicolas Sangouard.

* Electronic address: mikael.afzelius@unige.ch

- [1] Gisin, N. and Thew, R. Quantum communication. *Nat Photon* **1**, 165 (2007).
- [2] Gisin, N., Ribordy, G., Tittel, W., and Zbinden, H. Quantum cryptography. *Rev. Mod. Phys.* **74**, 145 (2002).
- [3] Bennett, C. H., Brassard, G., Crépau, C., Jozsa, R., Peres, A., and Wootters, W. K. Teleporting an unknown quantum state via dual classical and einstein-podolsky-rosen channels. *Phys. Rev. Lett.* **70**, 1895 (1993).
- [4] Kimble, H. J. The quantum internet. *Nature* **453**(7198), 1023 (2008).
- [5] Duan, L.-M., Lukin, M. D., Cirac, J. I., and Zoller, P. Long-distance quantum communication with atomic ensembles and linear optics. *Nature* **414**, 413 (2001).
- [6] Sangouard, N., Simon, C., de Riedmatten, H., and Gisin, N. Quantum repeaters based on atomic ensembles and linear optics. *arXiv:0906.2699* (2009).
- [7] Simon, C., de Riedmatten, H., Afzelius, M., Sangouard, N., Zbinden, H., and Gisin, N. Quantum repeaters with photon pair sources and multimode memories. *Phys. Rev. Lett.* **98**, 190503 (2007).
- [8] Hammerer, K., Sørensen, A., and Polzik, E. Quantum interface between light and atomic ensembles. *arXiv:0807.3358* (2008).
- [9] Sun, Y., Thiel, C. W., Cone, R. L., Equall, R. W., and Hutcheson, R. L. Recent progress in developing new rare earth materials for hole burning and coherent transient applications. *J. Lumin.* **98**, 281 (2002).
- [10] Longdell, J. J., Fraval, E., Sellars, M. J., and Manson, N. B. Stopped light with storage times greater than one second using electromagnetically induced transparency in a solid. *Phys. Rev. Lett.* **95**, 063601 (2005).
- [11] Chanelière, T., Matsukevich, D. N., Jenkins, S. D., Lan, S.-Y., Kennedy, T. A. B., and Kuzmich, A. Storage and retrieval of single photons transmitted between remote quantum memories. *Nature* **438**, 833 (2005).
- [12] Eisaman, M. D., André, A., Massou, F., Fleischhauer, M., Zibrov, A. S., and Lukin, M. D. Electromagnetically induced transparency with tunable single-photon pulses. *Nature* **438**, 837 (2005).
- [13] Choi, K. S., Deng, H., Laurat, J., and Kimble, H. J. Mapping photonic entanglement into and out of a quantum memory. *Nature* **452**, 67 (2008).
- [14] Julsgaard, B., Sherson, J., Cirac, J. I., Fiurášek, J., and Polzik, E. S. Experimental demonstration of quantum memory for light. *Nature* **432**, 482 (2004).
- [15] Nunn, J., Walmsley, I. A., Raymer, M. G., Surmacz, K., Waldermann, F. C., Wang, Z., and Jaksch, D. Mapping broadband single-photon wave packets into an atomic memory. *Phys. Rev. A* **75**, 011401 (2007).
- [16] Hosseini, M., Sparkes, B. M., Hétet, G., Longdell, J. J., Lam, P. K., and Buchler, B. C. Coherent optical pulse sequencer for quantum applications. *Nature* **461**, 241 (2009).
- [17] Moiseev, S. A. and Kröll, S. Complete reconstruction of the quantum state of a single-photon wave packet absorbed by a Doppler-broadened transition. *Phys. Rev. Lett.* **87**, 173601 (2001).
- [18] Kraus, B., Tittel, W., Gisin, N., Nilsson, M., Kröll, S., and Cirac, J. I. Quantum memory for nonstationary light fields based on controlled reversible inhomogeneous broadening. *Phys. Rev. A* **73**, 020302 (2006).

- [19] Hétet, G., Longdell, J. J., Alexander, A. L., Lam, P. K., and Sellars, M. J. Electro-optic quantum memory for light using two-level atoms. *Phys. Rev. Lett.* **100**, 023601 (2008).
- [20] Afzelius, M., Simon, C., de Riedmatten, H., and Gisin, N. Multimode quantum memory based on atomic frequency combs. *Phys. Rev. A* **79**, 052329 (2009).
- [21] de Riedmatten, H., Afzelius, M., Staudt, M. U., Simon, C., and Gisin, N. A solid-state light-matter interface at the single-photon level. *Nature* **456**, 773 (2008).
- [22] Simon, J., Tanji, H., Thompson, J. K., and Vuletic, V. Interfacing collective atomic excitations and single photons. *Phys. Rev. Lett.* **98**, 183601 (2007).
- [23] Zhao, B., Chen, Y.-A., Bao, X.-H., Strassel, T., Chu, C.-S., Jin, X.-M., Schmiedmayer, J., Yuan, Z.-S., Chen, S., and Pan, J.-W. A millisecond quantum memory for scalable quantum networks. *Nat Phys* **5**, 95 (2009).
- [24] Zhao, R., Dudin, Y. O., Jenkins, S. D., Campbell, C. J., Matsukevich, D. N., Kennedy, T. A. B., and Kuzmich, A. Long-lived quantum memory. *Nat Phys* **5**, 100 (2009).
- [25] Lan, S.-Y., Radnaev, A. G., Collins, O. A., Matsukevich, D. N., Kennedy, T. A., and Kuzmich, A. A multiplexed quantum memory. *Opt. Express* **17**, 13639 (2009).
- [26] Nunn, J., Reim, K., Lee, K. C., Lorenz, V. O., Sussman, B. J., Walmsley, I. A., and Jaksch, D. Multimode memories in atomic ensembles. *Phys. Rev. Lett.* **101**, 260502 (2008).
- [27] Chanelière, T., Ruggiero, J., Bonarota, M., Afzelius, M., and Le Gouët, J. L. Efficient light storage in a crystal using an atomic frequency comb. *arXiv:0902.2048* (2009).
- [28] Afzelius, M., Usmani, I., Amari, A., Lauritzen, B., Walther, A., Simon, C., Sangouard, N., Minář, J., de Riedmatten, H., Gisin, N., and Kröll, S. Demonstration of atomic frequency comb memory for light with spin-wave storage. *Phys. Rev. Lett.* **104**, 040503 (2010).
- [29] Amari, A., Walther, A., Sabooni, M., Huang, M., Kröll, S., Afzelius, M., Usmani, I., Lauritzen, B., Sangouard, N., de Riedmatten, H., and Gisin, N. Towards an efficient atomic frequency comb quantum memory. *arXiv:0911.2145* (2009).
- [30] Hesselink, W. H. and Wiersma, D. A. Picosecond photon echoes stimulated from an accumulated grating. *Phys. Rev. Lett.* **43**, 1991 (1979).
- [31] Carlson, N. W., Bai, Y. S., Babbitt, W. R., and Mossberg, T. W. Temporally programmed free-induction decay. *Phys. Rev. A* **30**, 1572 (1984).
- [32] Mitsunaga, M., Yano, R., and Uesugi, N. Spectrally programmed stimulated photon echo. *Opt. Lett.* **16**, 264 (1991).
- [33] Schwoerer, H., Erni, D., Rebane, A., and Wild, U. P. Subpicosecond pulse shaping via spectral hole-burning. *Opt. Commun.* **107**, 123 (1994).
- [34] Merkel, K. D. and Babbitt, W. R. Optical coherent-transient true-time-delay regenerator. *Opt. Lett.* **21**, 1102 (1996).
- [35] Tian, M., Reibel, R., and Babbitt, W. R. Demonstration of optical coherent transient true-time delay at 4 Gbits/s. *Opt. Lett.* **26**, 1143 (2001).
- [36] Macfarlane, R. M., Meltzer, R. S., Malkin, B. Z. Optical measurement of the isotope shifts and hyperfine and superhyperfine interactions of Nd in the solid state. *Phys. Rev. B* **58**, 5692 (1998).
- [37] Bertaina, S., Gambarelli, S., Tkachuk, A., Kurkin, I. N., Malkin, B., Stepanov, A., Barbara, B. Rare-earth solid-state qubits. *Nature Nanotechnology* **2**, 39 (2007).
- [38] Lauritzen, B., Minář, J., de Riedmatten, H., Afzelius, M., Sangouard, N., Simon, C., and Gisin, N. Telecommunication-wavelength solid-state memory at the single photon level. *arXiv:0908.2348* (2009).

Supplementary Information

We provide additional information for our manuscript. This material includes a detailed description of the experimental setup and of the atomic frequency comb preparation, as well as additional results.

Experimental details

Setup

The experimental setup is shown in Fig.7. The light is emitted by an external cavity diode laser (Toptica) at 883nm and is then split with a polarizing beam splitter (PBS) into two paths. In both paths, the amplitude, frequency and phase of the light can be modulated using acousto-optic modulators (AOM, AA-Opto-Electronics) in double pass configuration. The path on the top is used to prepare an AFC into the sample. To achieve this, the AOM creates a series of pulses with a characteristic spectrum explained in the next section. The other path is used to create the weak pulses of light at the single photon level that are going to be mapped onto the crystal. With an AOM and neutral density(ND) filters we create pulses containing less than one photon in average. The AOMs have a good extinction ratio (> 40 dB) and allows us to shift the frequency or the phase of the light. However, to create very short pulses(few ns), we use an additional a 20 GHz electro-optical modulator(EOM, EO Space).

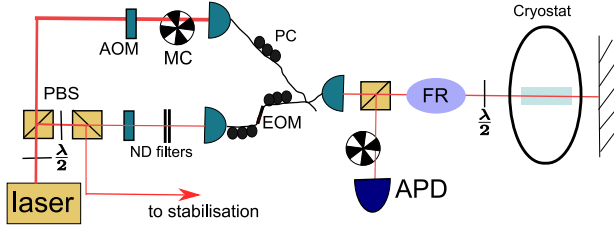


FIG. 7: Experimental setup : see text for details. The following abbreviations are used : polarizing beam splitter (PBS), acousto-optic modulator (AOM), neutral density filter(ND filter), mechanical chopper (MC), polarization controller (PC), electro-optical modulator (EOM), Faraday rotator (FR) and avalanche photo-diode (APD).

Both path are then combined using a 90/10 fiber coupler and sent into free space into the sample cooled at 3K using a pulse tube refrigerator (Oxford Instruments). The PBS combined to a $\lambda/2$ wave-plate allow us to adjust the polarization of the light parallel to the D1 crystallographic axis (optical axis). In order to increase the available optical depth, we implemented a double-pass setup using a Faraday Rotator(FR). In this way, we have a configuration where the polarization of the light remains constant when propagating in double pass through the crystal, but is rotated by 90 degrees after the second pass in the FR, such that the the light emitted by the crystal can be separated from the input light, thanks to a PBS.

The light is then coupled to a multimode optical fiber and detected by a single photon Si Avalanche Photo-Diode (APD) with 32% efficiency. The mechanical chopper(MC) in the preparation path is used to block the leakage of the preparation AOM when the APD is detecting echoes. The second MC is used to protect the APD when strong preparation pulses are used. The transmission between the input of the cryostat and the APD was typically between 25% and 30 %. Finally, a third path (partially shown), is used to actively frequency stabilize the laser to less than 100kHz using the Pound-Drever-Hall technique. The frequency reference is

given by a spectral hole in the crystal. The stabilization light is sent into the same sample, but with a slightly different angle.

The experiment is repeated every 200ms, allowing sufficient time for the ground state population to relax between experiments. The first 100ms were used for the preparation sequence to create an AFC. Then, we waited 5ms to avoid fluorescence during the storage and retrieval sequence, due to atoms left in the excited state after the preparation of the AFC. After that, we perform ~ 1000 independent storage trials separated by $5\mu s$. Each trial contains the particular pulse sequence to be stored and the re-emitted AFC echoes. Depending on the mean photon number per pulses, the total integration time to accumulate sufficient statistics varied from 30s to 10min.

Comb Preparation

We now explain in more detail the preparation sequence allowing us to create a desired AFC. Similarly to [1], we send series of pulses separated by a time τ , which create a periodicity of $\Delta = 1/\tau$ in the absorption profile. By sending repeatedly such sequence, this modulation will take the form of a comb with sharp peaks. However, instead of sending only pairs of pulses as in [1], we extended the method by allowing the possibility of sending N pulses. The spectrum of this series of N pulses is a a comb of periodicity $\Delta = 1/\tau$. However, we want to remove from the initial state only atoms that are not in the desired comb. The spectrum of the sequence must thus be the inverse of a comb : a series of holes separated by Δ . To achieve this, the central pulse must be π -dephased, and with a pulse area equal to the sum of the other pulses (see Fig.2).

The property of the comb can be determined by the characteristic of the pulses sequence. As already mentioned, the periodicity Δ is given by the time τ between pulses. The duration of one pulse(or its spectrum) will determine the bandwidth of the whole comb. Finally, the width of each peak will be inversely proportional to the duration of the whole pulse sequence. Similarly, we can say that the finesse of the comb will increase with the number of pulses ($F \sim N_{\text{pulses}}$). Note that these rules are true for the spectrum of the light, but the process of spectral hole burning being more complex, the property of the AFC can be different. For example, the width of each peak is limited by the crystal properties, such as homogeneous linewidth and superhyperfine interaction.

The comb preparation sequence for most of our experiments is shown in Fig.8. It takes $16\mu s$ and it is repeated around 2000 times. The available optical depth being relatively small ($d=3$), the optimal finesse to get the maximum storage end retrieval efficiency was about 3 [2]. It was thus sufficient to send only series of three pulses ($N=3$) to create the desired comb. The spectrum of the comb created in this way was around 20MHz. It was possible to extend this bandwidth by sending other series of pulses at a shifted frequency ($\pm 20\text{MHz}, \pm 40\text{MHz}, \text{etc.} \dots$). Since there is no interference between different frequencies, the pulses can be sent within the coherence time T_2 . This means that the whole preparation sequence take the same time as with a single frequency, and does not require more Rabi frequency.

Double read-out using double AFC

For the interference experiment, the stored excitations must be read-out at different times. For that purpose, we need to create multiple AFCs, with different periodicity Δ_i and possibly different phases. This can be realized by using a preparation pulse sequences with different pulse separations. Suppose that we want to create two AFCs with periodicity Δ_1 and Δ_2 . The necessary sequence is shown in Fig.9. We send a pulse sequence with N pulses separated by τ_1 (with the central pulse at $t=0$), superposed with N pulses separated by τ_2 (with the central pulse also at $t=0$). Thus, the total

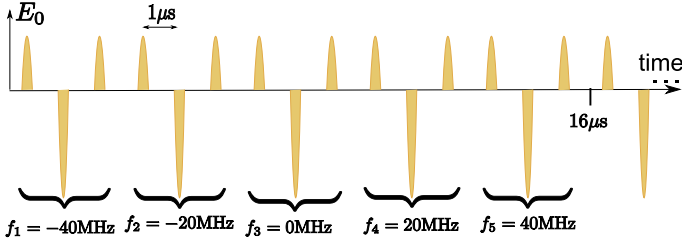


FIG. 8: Pulse sequence for atomic frequency comb preparation. In order to increase the bandwidth, the pulses are repeated with shifted frequencies. This pulse sequence was used for most of our experiments. Here it creates a comb of 100 MHz bandwidth and a periodicity of 1 MHz. The total sequence takes $16 \mu\text{s}$ and it is repeated around 2000 times in order to prepare the AFC.

number of pulses will be $2N-1$, and the pulse area of the central one is equal to the sum of the others. When we send a storage pulse in the sample, two echo will be emitted, after a time τ_1 and τ_2 . In our case, we use $N=3$, such that the total number of pulses for creating two AFCs with different periodicity is 5 (for one pumping frequency). Note that when we superpose two combs, some peaks of the two AFCs can be at the same position and be summed. This means that some peaks will be higher than others. Thus, using this method the two AFCs cannot be created independently (i.e. with two independent pulses series) or the absorption profile will not correspond to the sum of two AFCs and we will face additional echoes. So we must create directly two AFCs in one sequence.

Finally, we would like to be able to induce a phase ϕ in one of the AFCs, in other world to shift the frequency of the comb [2]. To do so, we must add a phase in each pulse preparing the corresponding comb (See Fig. 3). If we label the pulses on the right of the central one with $k=1,2,3\dots$ and the pulses on the left with $k=-1,-2,-3\dots$, then the phase in the pulse k must be $k\phi$.

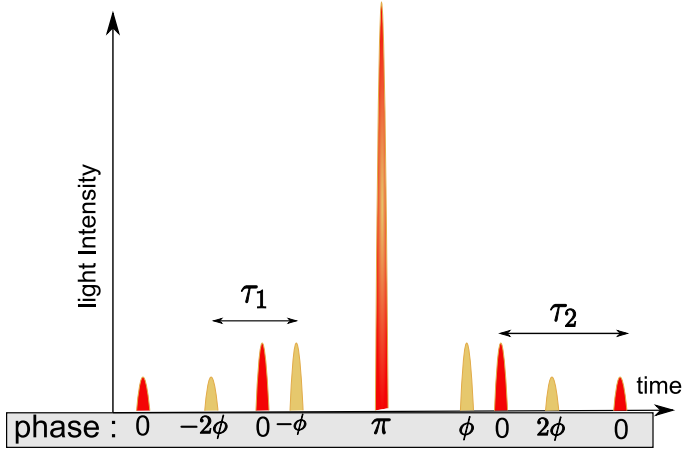


FIG. 9: Pulse sequence for the preparation of two atomic frequency combs, as required for the double read out for the interference experiments. In this example, the two AFCs have a periodicity $1/\tau_1$ and $1/\tau_2$. The first AFC will also get a phase ϕ .

Additional results

We present here some additional results that illustrate the multimode capacity of AFC. In Fig. 10 we show experimental combs

with 1 MHz peak separation (corresponding to $1 \mu\text{s}$ storage time) and 20 MHz and 100 MHz bandwidth, respectively. As noted, before the enlargement of the bandwidth does not affect the center of the comb. Thus it allows us to increase the number of mode for a fixed storage time without affecting the efficiency (see Fig.2 of the manuscript). However, compared to combs with bigger peak separation (shorter storage time), the height of the peaks has decreased, and the absorption background has increased, which explained the decay of efficiency with storage time. As explained in the paper, the number of mode is proportional to the number of peaks in the comb. Here we create more than 100 peaks which illustrate the multimode performance of our experiments.

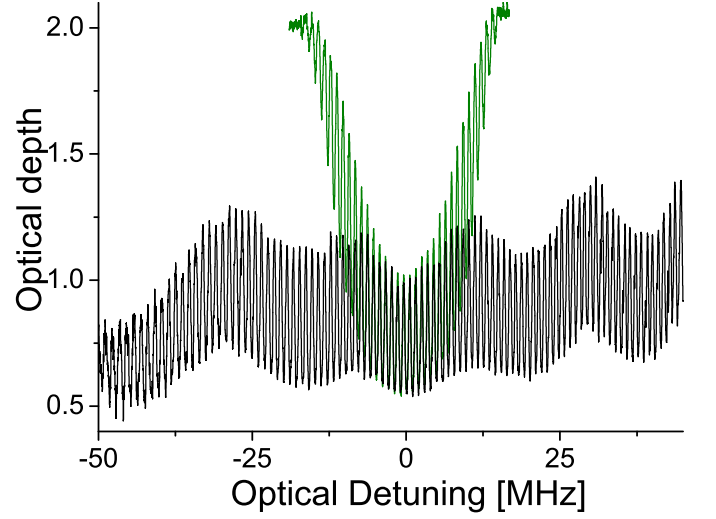


FIG. 10: Experimental atomic frequency combs with 1 MHz peak separation for single (green line) or five (black line) different simultaneous pump frequencies.

Finally, we show two more example of storage of 64 temporal modes with different inputs. In Fig.11, all the modes are full, which allows us in principle to store 32 time-bin qubits. In Fig.12, we modulated the amplitude of the input pulses. We note that even if the input mode changes, we do not need to adapt the AFC preparation. Indeed, the efficiency is constant for all modes, and the echo always closely follow the input pulses.

* Electronic address: mikael.afzelius@unige.ch

- [1] de Riedmatten, H., Afzelius, M., Staudt, M. U., Simon, C., and Gisin, N. A solid-state light-matter interface at the single-photon level. *Nature* **456**(7223), 773–777 December (2008).
- [2] Afzelius, M., Simon, C., de Riedmatten, H., and Gisin, N. Multimode quantum memory based on atomic frequency combs. *Phys. Rev. A* **79**(5), 052329–9 May (2009).

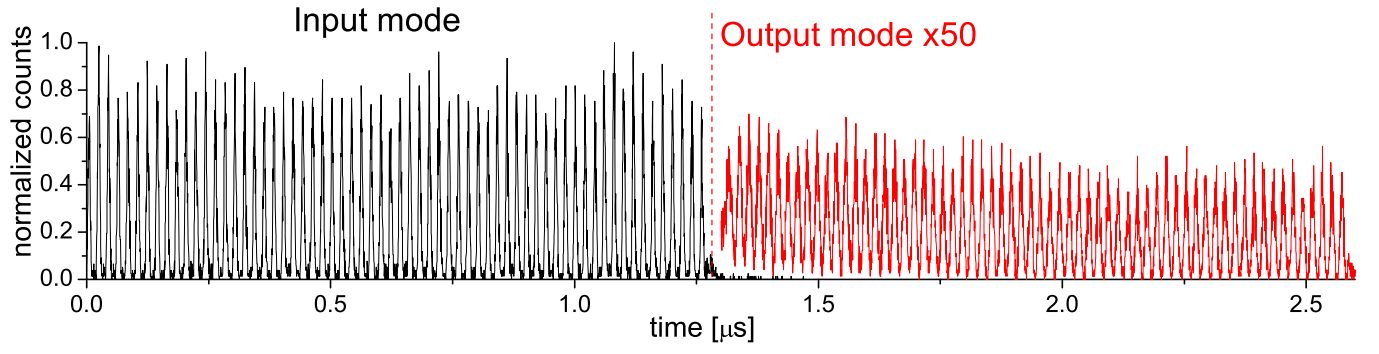


FIG. 11: Storage of 64 consecutive pulses. An efficiency of 1.4% was measured. The mean photon number per pulse is $\bar{n} \approx 0.5$

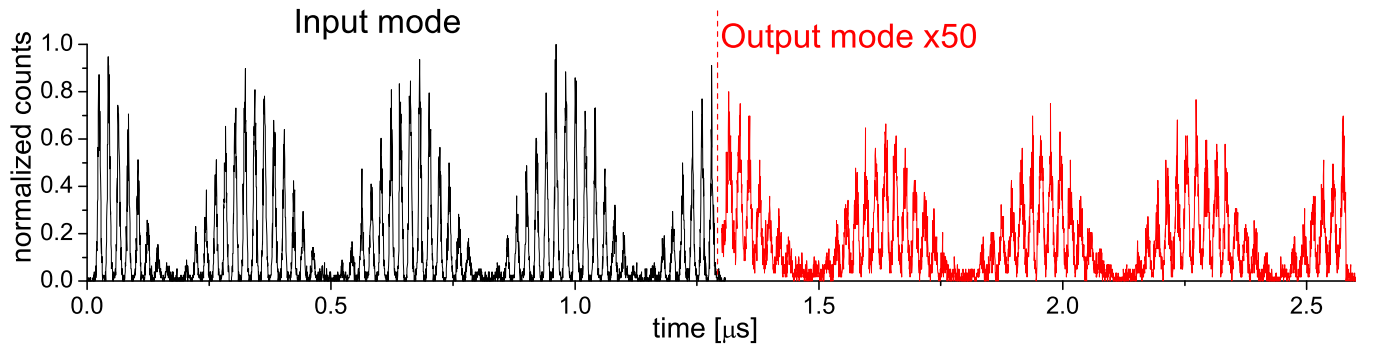


FIG. 12: Storage of 64 pulses with a modulating amplitude. An efficiency of 1.6% was measured. The mean photon number in the biggest pulses is $\bar{n} \approx 0.9$